j mater res technol. 2016;xxx(xx):xxx–xxx

Available online at www.sciencedirect.com

jmr&t Journal of Materials Research and Technology

www.jmrt.com.br

Original Article

Hot tensile properties and strain hardening behaviour of Super 304HCu stainless steel

M. Vinoth Kumar [a], V. Balasubramanian [b,*], A. Gourav Rao [c]

[a] Department of Mechanical Engineering, Hindustan Institute of Technology and Science, Hindustan University, Padur, Chennai, Tamil Nadu 603103, India

[b] Centre for Materials Joining and Research (CEMAJOR), Department of Manufacturing Engineering, Annamalai University, Annamalai Nagar, Tamil Nadu 608002, India

[c] Naval Materials Research Laboratory (NMRL), Ambernath, Mumbai 421506, India

ARTICLE INFO

Article history:
Received 12 August 2015
Accepted 17 May 2016
Available online xxx

Keywords:
Super 304HCu
High temperature tensile properties
Strain hardening behaviour
K–M plots

ABSTRACT

Super 304HCu austenitic stainless steel containing 2.3–3 (wt.%) of Cu is mainly used in superheaters and reheaters tubing of ultra super critical boilers which operates over 600 °C of steam temperature. Tensile tests were carried out on Super 304HCu, using nominal strain rate of $1 \times 10^{-3}\ s^{-1}$, at room temperature, 550 °C, 600 °C and 650 °C. The tensile strength and elongation were found to decrease with increase in test temperature. The stress strain curves were fitted using Hollomon equation to determine the strain hardening exponent value. Differential Crussard–Jaoul (C–J) analysis of the tensile curve is used to determine the variation in strain hardening exponent. Kocks–Mecking (K–M) type plots were used to determine the stages of strain hardening during tensile loading of the specimen. The strain hardening capacity of the Super 304HCu is found to decrease with increase in test temperature.

1. Introduction

Super 304HCu austenitic stainless steel (ASS) containing 2.3–3 (wt.%) of copper (Cu) is mainly used in superheaters and reheaters tubing of ultra super critical boilers which operates over 600 °C of steam temperature [1]. Super 304HCu belongs to 18% Cr–9% Ni system, with additions of Cu, Niobium, and Nitrogen, for precipitation strengthening. Cu is the distinct addition to this stainless steel in comparison to the others. Cu added to the steel provides better oxidation resistance, in addition to the precipitation of fine Cu rich phase during creep conditions and resulting in increased creep strength [2].

Sen et al. [3] investigated the microstructure and room temperature (RT) mechanical properties of 304H grade stainless steel with 3% Cu annealed at 700 °C up to 100 h. It was observed that the strength of the alloy remains unaltered after annealing, while the strain hardening exponent of the alloy enhances with annealing time. Yang et al. [4], Li et al. [5], Bai et al. [6] studied the ageing behaviour, microstructure evolution and precipitation behaviour of Super 304HCu boiler grade ASS and reported good microstructural and mechanical

* Corresponding author.
E-mail: visvabalu@yahoo.com (V. Balasubramanian).

http://dx.doi.org/10.1016/j.jmrt.2016.05.004

Please cite this article in press as: Vinoth Kumar M, et al. Hot tensile properties and strain hardening behaviour of Super 304HCu stainless steel. J Mater Res Technol. 2016. http://dx.doi.org/10.1016/j.jmrt.2016.05.004

Table 1 – Chemical composition (wt.%) of Super 304HCu austenitic stainless steel.

C	Si	Mn	P	S	Cr	Ni	N	Cu	Nb	B
0.086	0.23	0.81	0.021	0.0003	18.18	9.06	0.095	3.080	0.045	0.0039

stability of this alloy after exposure to high temperatures. Ha and Jung [7] studied the creep behaviour and microstructure evolution of Super 304HCu stainless steel at 750 °C in the stress range of 78–200 MPa. The creep behaviour and high temperature microstructural behaviour of this steel made it suitable for application in ultra super critical fossil power plants. Alaneme et al. [8] investigated the mechanical behaviour of 304H ASS containing 0–5 wt.% of Cu and found that the fracture behaviour was unaffected by Cu addition.

Tensile flow and work hardening behaviour attract significant scientific and technological interest with a view to optimize appropriate conditions for material processing and to ensure safe performance during service [9]. Work hardening behaviour, which influences strength and ductility, is one of the important considerations in evaluating the plastic deformation of materials [10]. A good number of semi-empirical relations are developed to describe the plastic flow behaviour of polycrystalline materials. The parameters involved in these constitutive equations have been used to investigate the underlying mechanisms and the change in microstructure that occur during deformation [11].

Though, the strain hardening behaviour of cubic metals is fairly well understood, and accumulation of a forest of dislocations is the predominant hardening mechanism [12]. From literature survey, it is found that few investigations were carried out on evaluating the mechanical properties of Super 304HCu at RT. However, the effect of test temperature on the strain hardening behaviour and the strain hardening stages, which may occur in Super 304HCu ASS, is scant and needs to be investigated. Hence, in this investigation an attempt has been made to study the effect of test temperature on tensile properties and strain hardening behaviour of Super 304HCu. Empirical relationships were used to describe the plastic flow behaviour.

2. Experimental details

Super 304HCu seamless tubes (Grade: DMV304HCu, Heat No. 100317) intended for use in heat exchangers of ultra super critical boilers were supplied by M/s Salzgitter Mannesmann Stainless Tubes Italia Srl, Italy. Tubes of outer diameter 57.1 mm and wall thickness of 3.5 mm were received in annealed condition (1145 °C), with ASTM grain size of 8. The chemical composition of Super 304HCu is given in Table 1 and the microstructure is shown in Fig. 1a, which

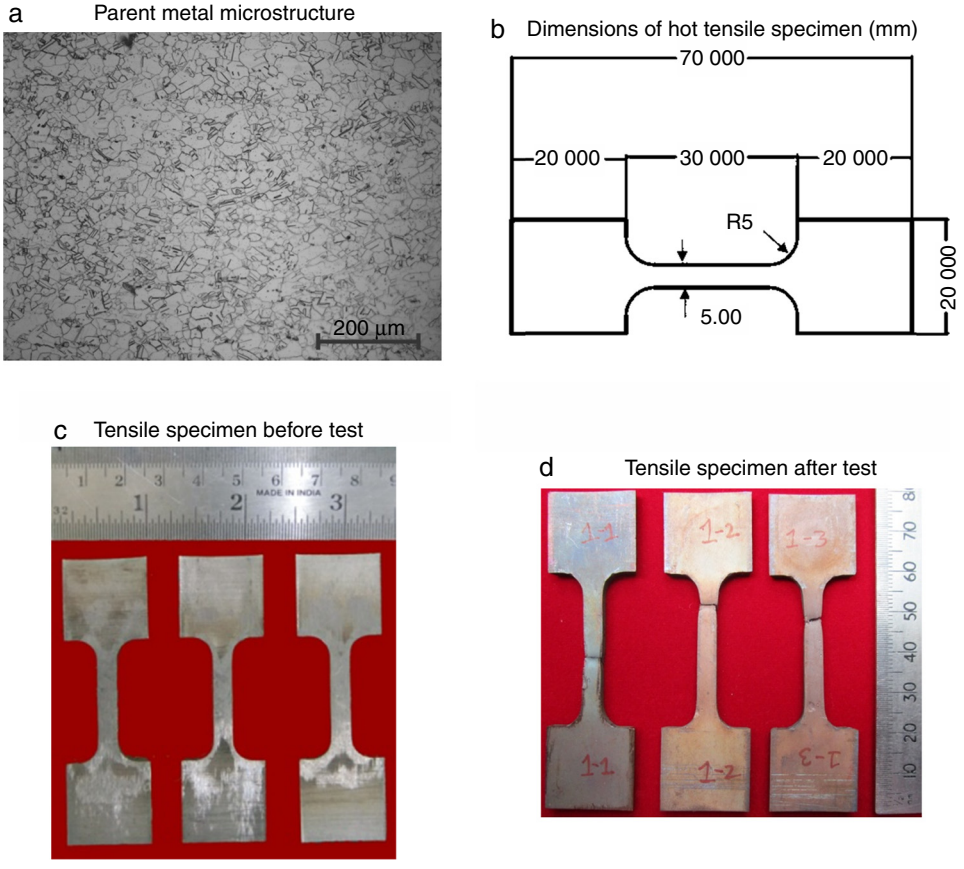

Fig. 1 – Optical microstructure and tensile specimen details.

Please cite this article in press as: Vinoth Kumar M, et al. Hot tensile properties and strain hardening behaviour of Super 304HCu stainless steel. J Mater Res Technol. 2016. http://dx.doi.org/10.1016/j.jmrt.2016.05.004

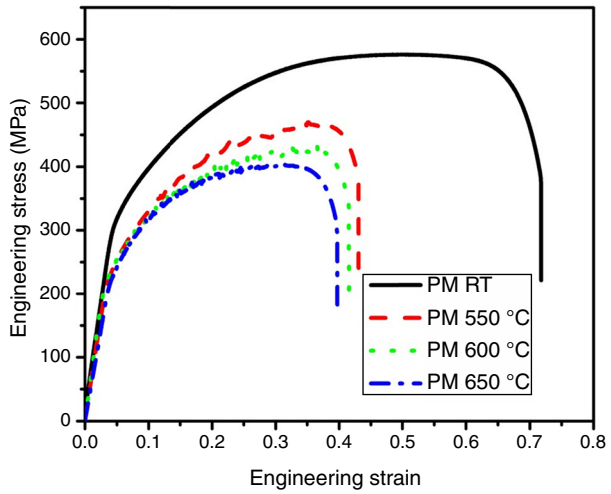

Fig. 2 – Engineering stress–strain curves at various test temperatures.

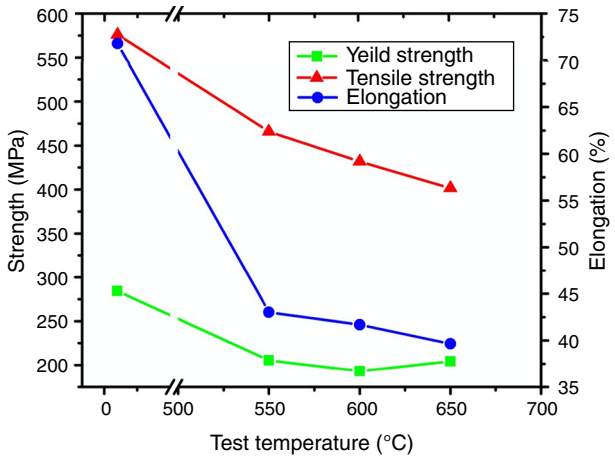

Fig. 3 – Effect of test temperature on strength and elongation.

consists of equiaxed austenitic grains with annealing twins. The schematic representation of hot tensile specimen with dimensions is shown in Fig. 1b.

Tensile tests were carried out using Instron universal testing machine (UTM) under the constant crosshead speed mode with a nominal strain rate of $1 \times 10^{-3}\,s^{-1}$. The tensile tests were carried out at test temperatures of RT, 550°, 600°, and 650 °C. The UTM was equipped with a three-zone resistance heating furnace for high temperature testing and a computer with data acquisition system for obtaining digital load-elongation data. The photographs of hot tensile specimens before and after test are shown in Fig. 1c and d, respectively. For microstructural examination using light optical microscope (OM) the specimens were prepared using standard metallographic techniques and etched with 3 parts HCL and 1 part HNO_3 for 5–10 s to reveal the microstructural features and for transmission electron microscope (TEM) thin film specimen were suitably prepared. The fracture surfaces of the tensile specimens were analyzed using scanning electron microscope (SEM) to reveal the mode of fracture.

3. Results

3.1. *Tensile properties*

Engineering stress–strain curves of Super 304HCu tested at various temperatures are shown in Fig. 2 and their tensile properties are presented in Table 2. The effect of test temperature on tensile strength, yield strength and elongation are shown in Fig. 3. The tensile strength and elongation decreases, with increase in test temperature from RT to 650 °C. However the decrease in elongation from RT to 550 °C was 28.8%, and within the temperature range of 550 °C to 650 °C the decrease is marginal.

3.2. *Strain hardening capacity*

The hardening capacity (H_c) of a material may be considered as a ratio of the ultimate tensile strength (σ_{UTS}), to the yield strength (σ_y) [13,14]. Afrin et al. [13] modified the hardening capacity to a normalized parameter as,

$$H_c = \frac{\sigma_{UTS} - \sigma_y}{\sigma_y} = \frac{\sigma_{UTS}}{\sigma_y} - 1 \quad (1)$$

The H_c of Super 304HCu at different test temperatures is presented in Table 2. H_c increased with the increase in test temperature from RT to 550 °C. On further increase in test temperature between 550 °C to 650 °C the H_c decreased.

3.3. *Strain hardening behaviour*

The strain hardening exponent is a measure of the ability of a metal to strain harden; the larger its magnitude, the greater the strain hardening for a given amount of plastic strain [15]. The larger the n value, the more the material can deform before instability, and the material can be stretched further before necking starts [16]. The tensile test data in the

Table 2 – Tensile properties of Super 304HCu austenitic stainless steel at different test temperatures.

Test temperature (° C)	0.2% Yield strength (MPa)	Ultimate tensile strength (MPa)	Elongation in gauge length of 25 mm (%)	Strain hardening capacity 'H_c'
RT	284.2	575.8	71.8	1.03
550	205.5	465.8	43.0	1.27
600	193.0	431.8	41.7	1.24
650	204.3	401.8	39.6	0.97

Please cite this article in press as: Vinoth Kumar M, et al. Hot tensile properties and strain hardening behaviour of Super 304HCu stainless steel. J Mater Res Technol. 2016. http://dx.doi.org/10.1016/j.jmrt.2016.05.004

Table 3 – Strain hardening exponent values of Super 304HCu austenitic stainless steel tested at various temperature.

Test temperature (° C)	Hollomon		C–J analysis	
	(n_1^H)	(n_2^H)	$(n_1^{CJ}-1)$	$(n_2^{CJ}-1)$
RT	0.07	0.28	−0.23	−0.83
550	0.12	0.34	−0.12	−0.91
600	0.11	0.33	−0.37	−0.99
650	0.14	0.27	−1.35	−0.38

region of uniform plastic deformation was fitted using the empirical Hollomon's equation [17] $\sigma = k\varepsilon^n$ to determine the strain hardening exponent 'n' where, n is the strain hardening exponent, k is the strength coefficient, σ is the true stress and ε is the true strain. Fig. 4a shows the log–log plot of true stress–true plastic strain at different test temperatures, where the slope of this plot represents the 'n' value. From the plot, two stages of strain hardening were identified, each

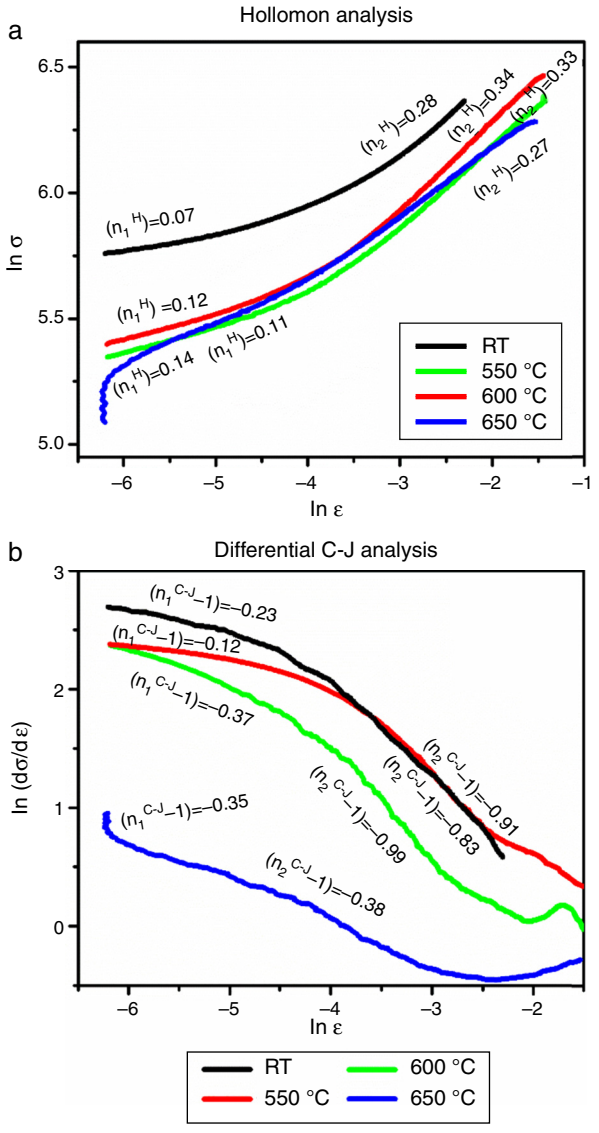

Fig. 4 – Determination of strain hardening exponent of Super 304HCu tested at different temperature.

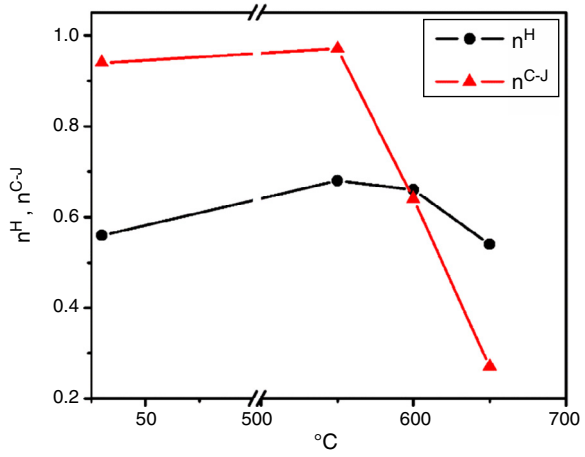

Fig. 5 – Effect of test temperature on strain hardening exponent determined using Hollomon and differential C–J analysis.

having its own 'n' value. The value of the two 'n' obtained from the Hollomon's equation is given as n_1^H and n_2^H in Table 3, where n_1^H represents the slope of the low strain region and n_2^H represents the slope of high strain region.

In order to quantify the strain hardening response better, differential Crussard–Jaoul (C–J) analysis [18] of the tensile curve is used to determine the variation in strain hardening exponent. Assuming Ludwik power relationship [19], $\sigma = \sigma_y + k_1\varepsilon^n$, where n is the strain-hardening exponent, σ_y is the yield stress and, k is the strength coefficient. After differentiation with respect to ε, a log–log plot $(d\sigma/d\varepsilon) - \varepsilon$, shown in Fig. 4b reveals a linear plot with the slope gives value of '$(n^{CJ}-1)$'. The value of '$(n^{CJ}-1)$' obtained at various test temperatures is listed in Table 3. The value of n_2^H and n_2^{CJ} is considered to be more sensitive to test temperatures, as the strain hardening exponent usually tends to decrease with increase in test temperature. The n_1^H value being lower, shows increasing trend with increase in temperature is considered to be less sensitive to temperature. The effect of test temperature on strain hardening exponents (n^H and n^{CJ}) are shown in Fig. 5. Similar results were reported by Afrin et al. [13] and Chowdhury et al. [20].

3.4. *Strain hardening rate*

In order to understand the work-hardening behaviour of the steels, the instantaneous work-hardening rate $\theta = d\sigma/d\varepsilon$ is considered [21,22]. Kocks–Mecking (KM) plot of strain-hardening rate (θ) as a function of net flow stress $(\sigma - \sigma_y)$ has been widely used to interpret tensile work hardening behaviour of metals and alloys [20]. The KM plot at different test temperature is shown in Fig. 6. Stage I and stage II hardening is not observed for Super 304HCu at all test temperature. Stage II hardening is usually weakly sensitive or insensitive to temperature and strain rate. Following stage II, typical stage III results in a continuous and linear decrease in the work hardening rate that depends on applied strain rate and temperature. As stage III approaches to a saturation level, stage IV appears at large strains. Stage IV is characterized by the low

Please cite this article in press as: Vinoth Kumar M, et al. Hot tensile properties and strain hardening behaviour of Super 304HCu stainless steel. J Mater Res Technol. 2016. http://dx.doi.org/10.1016/j.jmrt.2016.05.004

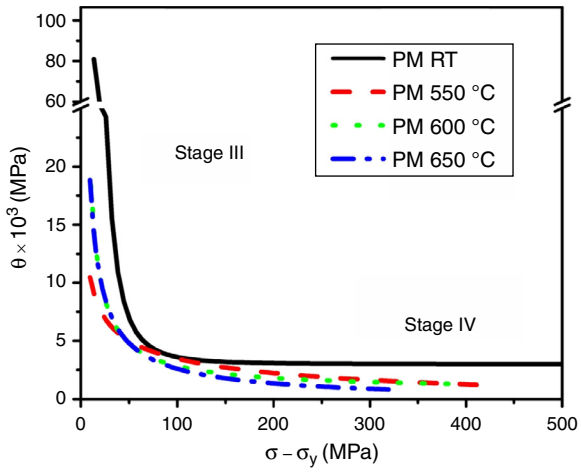

Fig. 6 – K–M plot of strain hardening rate (θ) vs. net flow stress ($\sigma - \sigma_y$).

and nearly constant work hardening rate [9]. The stage III and stage IV strain hardening was observed, and it is sensitive to variation in the test temperature. From Fig. 6, it is observed that the K–M plots shift to lower stresses, i.e. shifts towards the origin with increase in temperature. However a transition at 600 °C is observed with the plots for temperatures 600 °C and 650 °C being shifted to high stress region during the beginning of stage III, with an increase in initial strain hardening rates. In case of region IV, with increase in test temperature the strain hardening rate has decreased. Further, a steady reduction in length of region IV has been observed with increase in test temperature.

3.5. *Fracture surfaces*

Fracture surface of the specimens tested at RT and 650 °C are shown in Fig. 7(a and b) respectively. The fracture was considered to be completely ductile in case of RT test, with voids of varying sizes surrounded by fine dimples, voids are associated with the precipitates present in the austenitic matrix (refer Fig. 7a). The fracture surface of specimens tested at high temperature reveals fewer voids, much larger in size and cleavage like featureless facets than the specimen tested at RT [20]. It is evident from the fractographs that the fracture at high temperature is more brittle than at RT. The more brittle nature of failure in high temperature test is evidenced by the constant decrease in elongation of the specimens with increase in test temperature; similar results were reported by Farabi et al. [23]. However, the fracture surface of specimen tested at all temperatures invariably consists of dimples of varying sizes, evidencing the predominantly ductile mode of failure, with voids attributed to the sites of precipitates, which act as crack initiation points.

4. Discussion

Stress–strain curves of Super 304HCu tested at various temperatures exhibit continuous yielding behaviour (refer Fig. 2). The continuous yielding has been related to the presence of mobile dislocations during the initial stages of plastic deformation, which are created in austenite matrix via plastic deformation [24]. In a way, the tensile hardening capacity of the material may be related to the strength of the material in terms of H_c, it has a direct relationship with the material's strength [25]. In this work, the H_c represents the material's ability to harden during tensile loading in the region from YS to UTS. Super 304HCu at RT is less likely to harden, than tested at high temperatures up to 600 °C. However, the hardening capacity decreases at the test temperature of 650 °C. Hardening capacity of FCC metals is mainly governed by the dislocation–dislocation interaction rather than the grain boundary strengthening dependent on the grain size [26]. The annihilation of dislocation increases with increase in test temperature from 550 to 650 °C and hence the hardening capacity decreases. At lower temperature the lattice resistance to the dislocation motion is higher and hence the strength at lower temperature is higher than the high temperature strength.

The yield strength, tensile strength, and strain hardening rate of Super 30HCu decrease with increase in temperature. Strain hardening arises from the blockade in dislocation motion at a barrier, the obstacle may be a grain boundary, sub-grain boundary, tangled cell, second phase, etc. Two strain hardening stages were observed in the Hollomon fit of tensile curve represents that n_1^H is sensitive to the matrix, whereas the n_2^H is sensitive to the second phase particles, i.e., the precipitates in the matrix. Similar results were reported by Zhang et al. [27] and proposed a single parameter, mean free path (MFP) of dislocation motion, as a measure to account for the

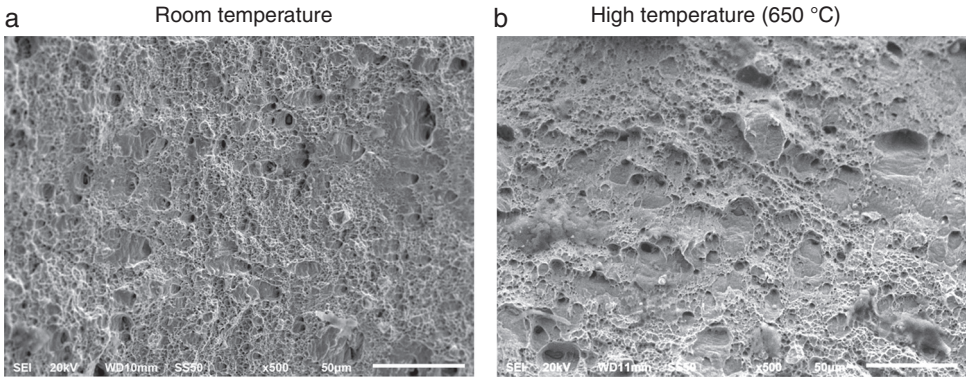

Fig. 7 – Fracture surface of Super 304HCu tensile specimens.

Please cite this article in press as: Vinoth Kumar M, et al. Hot tensile properties and strain hardening behaviour of Super 304HCu stainless steel. J Mater Res Technol. 2016. http://dx.doi.org/10.1016/j.jmrt.2016.05.004

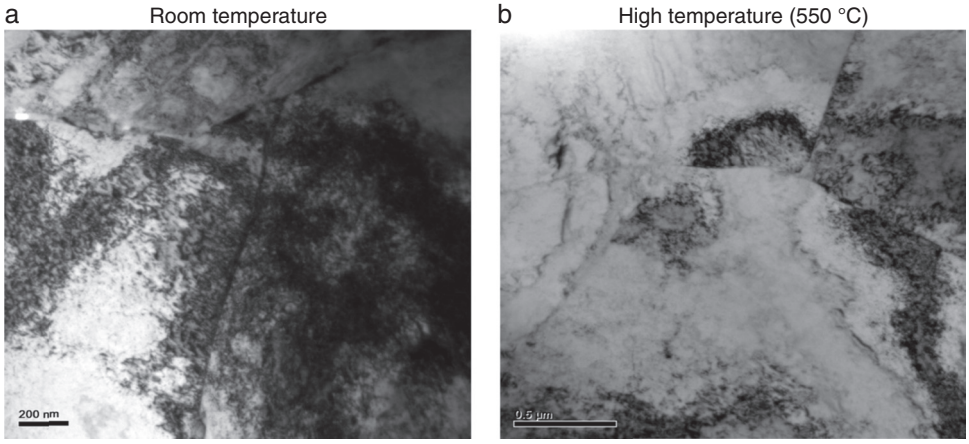

Fig. 8 – Transmission electron micrograph of Super 304HCu tensile specimens.

strain hardening, is equal to the grain size, sub-grain size, and interparticle spacing of the second phases. The MFP of dislocation decreases with increase in dislocation density and results in a decrease of instantaneous strain hardening exponent. The decrease in value of $(n_1^{CJ} - 1)$ from 550 °C to 650 °C represents the amount of dislocation annihilation. The higher value of $(n_1^{CJ} - 1)$ for 650 °C determined from C–J analysis indicate the rapid recovery process occurred at this temperature.

From the K–M plot, the θ decreases continuously and becomes almost constant (refer Fig. 6), indicating the stage III and stage IV behaviour of strain hardening. The stage III is characterized by simultaneous storage and the annihilation of dislocations, whereas the stage IV is merely a dislocation storage process. Regardless of the temperature the dislocations are stored and annihilated after reaching a critical stress or/and strain. The annihilation increases with increase of stress until an equilibrium between the storage and annihilation of dislocations is achieved, leading to stage IV with constant dislocation density at constant stress [28]. TEM micrographs of tensile specimen tested at RT and 550 °C shown in Fig. 8, reveals the annihilation of dislocations at higher temperatures (refer Fig. 8b). The increase in test temperature lead to lowering of initial θ values and lower θ values at the stage IV of strain hardening. Stage III is termed as "dynamic recovery" described by the decreasing slope of strain hardening rate in the K–M plot and is very sensitive to the temperature. Stage III is strongly dependent on the material and its stacking fault energy. The decrease in the hardening rate with strain is strongly dependent on temperature, indicating the need for a stress-dependent activation energy [29]. Steeper decrease of θ in stage III for all test temperatures, results in decreased strength.

The strain hardening behaviour can be explained by the dislocation theory of strain hardening [30]. The decrease in the strain hardening rate at stage III indicates the dominant role of dislocation annihilation, rather than dislocation–dislocation interaction and multiplication. The extremely high initial hardening rate may be related to the simultaneous resistance offered by the large amount of defect sources, such as twin boundaries [14]. At high temperatures, a rapid shift in K–M plots (refer Fig. 6) to lower stresses with increasing temperature indicates the dominance of recovery processes leading to early cross-slip and climb of dislocations. It is suggested that the initial work-hardening rate, to be temperature independent. The change in initial work hardening rate can be associated with change in controlling deformation mechanisms from RT to high temperatures [31]. In particular, stage III is sensitive to microstructure, dislocation annihilation, contributes to the decrease in strain hardening.

The difference in respective work hardening parameters with increase in temperature from room to high temperatures suggests that the dislocation sub-structural behaviour in its totality is different in the two temperature regimes. At higher temperatures, significant reduction in strength with increase in temperature indicates the acceleration in recovery processes [32]. The thermal activation available at high temperature may also contribute to the low work hardening rate at high temperatures. However, the change of yield strength and crossover of stress–strain curves in certain region may be related to the texture effect or intrinsic work hardening effects [29].

5. Conclusions

1. The yield strength, tensile strength and elongation of Super 304HCu decrease with increase in test temperature. The strain hardening capacity (H_c) of the material increases up to 600 °C and decreases at 650 °C.
2. Hollomon empirical relationship used to fit the stress–strain curves, represented 2 hardening stages, each having its own strain hardening exponent value. Differential Crussard–Jaoul (C–J) analysis of tensile curve of Super 304HCu revealed the lowering of strain hardening exponent value with increase in test temperature.
3. The K–M plots for all test temperatures were characterized by two stage hardening behaviour, with stage III represented by a rapid decrease in strain hardening rate followed by stage IV with relatively constant strain hardening rate. K–M plots of Super 304HCu shift to lower stresses, with increase in temperature, indicating that the material is temperature sensitive to tensile hardening.

Please cite this article in press as: Vinoth Kumar M, et al. Hot tensile properties and strain hardening behaviour of Super 304HCu stainless steel. J Mater Res Technol. 2016. http://dx.doi.org/10.1016/j.jmrt.2016.05.004

4. The accelerated recovery and availability of thermal activation at high temperature contributed to the low work hardening rate at high temperatures.

Conflicts of interest

The authors declare no conflicts of interest.

Acknowledgements

The authors wish to express their sincere thanks to M/s Mailam India Ltd., Pondicherry, India for providing fund to carry out this research work through the Mailam India Research (MIR) Fellowship, M/s Salzgitter Mannesmann Stainless Tubes Italia Srl, Italy for supplying the Super 304HCu tubes required to carry out this work and Naval Materials Research Laboratory (NMRL), Ambernath, Mumbai for providing the hot tensile testing facility.

REFERENCES

[1] Viswanathan R, Bakker WT. Materials for ultra supercritical fossil power plants. EPRI Technical report TR-114750; 2000.
[2] Chi C, Yu H, Xie X. Advanced austenitic stainless steel for ultra-supercritical (USC) fossil power plants. In: Morales EV, editor. Alloy steel properties and use. China: Intech; 2011. p. 171–202.
[3] Sen I, Amankwah E, Kumar NS, Fleury E, Oh ishi K, Hono K, et al. Microstructure and mechanical properties of annealed SUS 304H austenitic stainless steel with copper. Mater Sci Eng A 2011;528:4491–9.
[4] Yang H, Peng F, Miao X, Yang X. Investigation of the aging behavior on boiler steel tube super304H. Press Equip Syst 2006;4:96–9.
[5] Li XM, Zou Y, Zhang ZW, Zou Z-D. Microstructure evolution of a novel super 304H steel aged at high temperatures. Mater Trans 2010;51:305–9.
[6] Bai JW, Liu PP, Zhu YM, Li XM, Chi CY, Yu HY, et al. Coherent precipitation of copper in super 304H austenite steel. Mater Sci Eng A 2013;584:57–62.
[7] Ha VT, Jung WS. Creep behavior and microstructure evolution at 750 °C in a new precipitation strengthened heat resistant austenitic stainless steel. Mater Sci Eng A 2012;558:103–11.
[8] Alaneme KK, Hong SM, Indrani Sen Fleury E, Ramamurty U. Effect of copper addition on the fracture and fatigue crack growth behavior of solution heat-treated SUS 304H austenitic steel. Mater Sci Eng A 2010;527:4600–4.
[9] Choudhary BK, Christopher J, Isaac Samuel E. Applicability of Kocks–Mecking approach for tensile work hardening in P9 steel. Mater Sci Technol 2012;28:644–50.
[10] Karami M, Mahmudi R. Work hardening behavior of the extruded and equal-channel angularly pressed Mg-Li-Zn alloys under tensile and shear deformation modes. Mater Sci Eng A 2014;607:512–20.
[11] Akbarpour MR, Ekrami A. Effect of ferrite volume fraction on work hardening behavior of high bainite dual phase (DP) steels. Mater Sci Eng A 2008;477:306–10.
[12] Wang SQ, Liu JH, Chen DL. Effect of strain rate and temperature on strain hardening behavior of a dissimilar joint between Ti-6Al-4V and Ti17 alloys. Mater Des 2014;56:174–84.
[13] Afrin N, Chen DL, Cao X, Jahazi M. Strain hardening behavior of a friction stir welded magnesium alloy. Scr Mater 2007;57:1004–7.
[14] Luo J, Mei Z, Tian W, Wang Z. Diminishing of work hardening in electroformed polycrystalline copper with nano-sized and uf-sized twins. Mater Sci Eng A 2006;441:282–90.
[15] Callister WD Jr. Materials science and engineering-an introduction. 8th Ed. New York: John Wiley & Sons Inc.; 2009.
[16] Movahed P, Kolahgar S, Marashi SPH, Pouranvari M, Parvina N. The effect of intercritical heat treatment temperature on the tensile properties and work hardening behavior of ferrite–martensite dual phase steel sheets. Mater Sci Eng A 2009;518:1–6.
[17] Hollomon JH. Trans AIME 1945;162:268.
[18] Cussard CH, Jaoul B. Rev Met 1950;57:589.
[19] Ludwik P. Elemente der Technologischen Mechanik. Berlin: Springer-Verlag; 1909.
[20] Chowdhury SM, Chen DL, Bhole SD, Cao X, Powidajko E, Weckman DC, et al. Tensile properties and strain-hardening behavior of double-sided arc welded and friction stir welded AZ31B magnesium alloy. Mater Sci Eng A 2010;527:2951–61.
[21] Mecking H, Kocks UF. Kinetics of flow and strain hardening. Acta Metall Mater 1981;29:1865–75.
[22] Christopher J, Choudhary K, Isaac Samuel E, Srinivasan VS, Mathew MD. Tensile flow and work hardening behaviour of 9Cr-1Mo ferritic steel in the frame work of Voce relationship. Mater Sci Eng A 2011;528:6589–95.
[23] Farabi N, Chen DL, Zhou Y. Microstructure and mechanical properties of laser welded dissimilar DP600/DP980 dual phase steel joints. Alloys Compd 2011;509:982–9.
[24] Lian J, Jiang Z, Liu J. Theoretical model for the tensile work hardening behaviour of dual-phase steel. Mater Sci Eng A 1991;147:55–65.
[25] Zhu ML, Wang DQ, Xuan FZ. Effect of long term aging on microstructure and local behavior in the heat-affected zone of a Ni-Cr-Mo-V steel welded joint. Mater Charact 2014;87:45–61.
[26] Sun PL, Cerreta PK, Gray GT III, Bingert JF. The effect of grain size strain rate and temperature on the mechanical behavior of commercial purity aluminum. Metall Mater Trans A 2006;37A:2983–94.
[27] Fan Z, Mingzhi H, Deke S. The relationship between the strain-hardening exponent n and the microstructure of metals. Mater Sci Eng A 1989;122:211–3.
[28] Zehetbauer M, Seumer V. Cold work hardening in stages iv and v of FCC metals – experiments and interpretation. Acta Metall Mater 1993;41:577–88.
[29] Kocks UF, Mecking H. Physics and phenomenology of strain hardening: the FCC case. Prog Mater Sci 2003;48:171–273.
[30] Khodaverdizadeh H, Mahmoudi A, Heidarzadeh A, Nazari E. Effect of friction stir welding (FSW) parameters on strain hardening behavior of pure copper joints. Mater Des 2012;35:330–4.
[31] Choudhary BK, Rao Palaparti DP, Isaac Samuel E. Analysis of tensile stress–strain and work-hardening behavior in 9Cr-1Mo ferritic steel. Metall Mater Trans A 2013;44a:212–23.
[32] Choudhary BK, Rao Palaparti DP. Comparative tensile flow and work hardening behaviour of thin section and forged thick section 9Cr-1Mo ferritic steel in the framework of Voce equation and Kocks–Mecking approach. Nucl Mater 2012;430:72–81.

Please cite this article in press as: Vinoth Kumar M, et al. Hot tensile properties and strain hardening behaviour of Super 304HCu stainless steel. J Mater Res Technol. 2016. http://dx.doi.org/10.1016/j.jmrt.2016.05.004